

Novel type of ferroelectricity in brownmillerite structures: A first-principles study

Hao Tian,^{1,2,3} Xiao-Yu Kuang,¹ Ai-Jie Mao,^{1,*} Yurong Yang,^{2,3,†} Hongjun Xiang,^{2,4} Changsong Xu,² S. Omid Sayedaghaee,⁵ Jorge Íñiguez,⁶ and L. Bellaiche^{2,‡}

¹*Institute of Atomic and Molecular Physics, Sichuan University, Chengdu 610065, China*

²*Physics Department and Institute for Nanoscience and Engineering, University of Arkansas, Fayetteville, Arkansas 72701, USA*

³*National Laboratory of Solid State Microstructures, College of Engineering and Applied Sciences, and Collaborative Innovation Center of Advanced Microstructures, Nanjing University, Nanjing 210093, China*

⁴*Department of Physics, Key Laboratory of Computational Physical Sciences (Ministry of Education), State Key Laboratory of Surface Physics, Fudan University, Shanghai 200433, China*

⁵*Microelectronics-Photonics Program and Physics Department, University of Arkansas, Fayetteville, Arkansas 72701, USA*

⁶*Materials Research and Technology Department, Luxembourg Institute of Science and Technology (LIST), 5 Avenue des Hauts-Fourneaux, L-4362 Esch/Alzette, Luxembourg*



(Received 24 January 2018; published 7 August 2018)

First-principles calculations are conducted on two magnetic brownmillerites, namely, $\text{Ca}_2\text{Co}_2\text{O}_5$ and $\text{Sr}_2\text{Co}_2\text{O}_5$. Both systems possess a previously overlooked polar $Pmc2_1$ phase that is low in energy. This ferroelectric state is even predicted to be the ground state of $\text{Sr}_2\text{Co}_2\text{O}_5$, which therefore renders such material multiferroic. Strikingly, the ferroelectricity associated with this $Pmc2_1$ phase involves an original energetic coupling that is linear in the polar mode, quadratic in another distortion, and linear in a third mode. Such ferroelectricity is therefore of a novel type, since it differs from previously reported proper, improper, hybrid improper, and triggered kinds of ferroelectricity.

DOI: [10.1103/PhysRevMaterials.2.084402](https://doi.org/10.1103/PhysRevMaterials.2.084402)

I. INTRODUCTION

Brownmillerite (BM) oxides form a special class of materials that share the $A_2B_2O_5$ stoichiometry, where A and B are cations. They can be thought to be derived from the common ABO_3 perovskite oxides by replacing 1/6 of oxygen ions by vacancies. Several recent studies have been devoted to brownmillerite oxides [1–8] and have pointed out their potential interest and the possibility that they might present novel phenomena. For instance, a topotactic phase transformation from brownmillerite to perovskite was demonstrated via oxygen storage and release, and provides an effective means for a reversible oxidation and reduction process [6–8]. A reversible and nonvolatile electric-field control of a tristate phase transformation (involving brownmillerite, perovskite and another structure) by a selective dual-ion switch was also recently achieved, inducing striking electrochromic and magnetoelectric effects [9]. Furthermore, room-temperature electric-field control of ferromagnetism through oxygen-ion gating was also demonstrated via the use of brownmillerites [10].

Due to the fact that BM oxides have been much less studied than their perovskite counterparts, it is pertinent to ask if other interesting effects await to be discovered in $A_2B_2O_5$ compounds, especially noting that Ref. [11] revealed that metallic and ferromagnetic $(\text{La}_{1/2}\text{Ba}_{1/2})\text{CoO}_3$ perovskite can become insulating, antiferromagnetic, and even polar when adopting

the $(\text{La}, \text{Ba})\text{Co}_2\text{O}_5$ stoichiometry. For instance, one may wonder if a previously overlooked polar phase(s) can exist in some $A_2B_2O_5$ brownmillerites for which B is a magnetic ion, which will render such systems multiferroic—which is of obvious interest when recalling that multiferroics are scarce while having a large technological potential [12–15]. If such a hypothetical novel polar phase does exist in BM oxides, one would like to determine the nature of its electrical polarization. In other words, is it solely due to an intrinsic polar instability or rather induced by energetic coupling with other modes? If it is the latter, what are these modes, how many are there, and what is the analytical form of this energetic coupling? In other words, are BM oxides proper ferroelectrics or rather improper [16], hybrid improper [17–22], or even triggered-type ferroelectrics [23,24]?

Motivated to resolve these issues, we performed first-principles calculations on two representative compounds of magnetic brownmillerite oxides, namely, $\text{Ca}_2\text{Co}_2\text{O}_5$ and $\text{Sr}_2\text{Co}_2\text{O}_5$. It is presently reported that both of these materials do possess a previously overlooked polar phase of low energy, this phase being predicted to be the ground state of $\text{Sr}_2\text{Co}_2\text{O}_5$. Moreover and strikingly, the analysis of our *ab initio* computations reveals that the resulting ferroelectricity of such overlooked phases is of a new type, since it involves an original coupling involving the polar distortion (linearly) and two nonpolar modes that appear with quadratic and linear dependencies, respectively.

II. METHODS

As detailed in the Supplemental Material (SM) [25], we conducted density functional theory calculations [26] within the revised Perdew, Burke, and Ernzerhof functional for solids

*scu_mij@126.com

†yyrwater@uark.edu

‡laurent@uark.edu

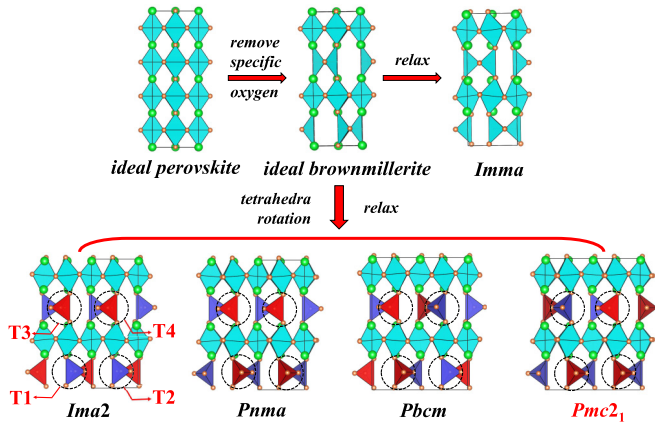


FIG. 1. Schematization of the construction of the ideal brownmillerite structure from the ideal perovskite structure and resulting relaxations allowing for the formation of the high-symmetry *Imma* state as well as for lower-in-symmetry *Ima2*, *Pnma*, *Pbcm*, and *Pmc2₁* phases of brownmillerites. The tilting pattern of the T1, T2, T3, and T4 oxygen tetrahedra (see text) is emphasized for each of these low-symmetry phases, with red and blue colors representing clockwise and anticlockwise rotation about the *z* axis, respectively.

plus the Hubbard parameter U (PBEsol + U), with $U = 2.5$ eV for Co ions [11,27]. We also considered spin arrangements that are most common in perovskites, namely, ferromagnetic (FM), A-type antiferromagnetic (A-AFM), C-type antiferromagnetic (C-AFM), and G-type antiferromagnetic (G-AFM). As shown in the SM [25], the G-AFM ordering is numerically found to present the lowest energy in our investigated systems and phases, which is in line with previous works [28,29]. We will thus adopt such ordering in the results shown here.

III. RESULTS

As indicated in the top left of Fig. 1, we start from the ideal perovskite cubic structure and remove one-sixth of its oxygen ions to build the high-symmetry *Imma* brownmillerite phase. Note that such removal results in the formation of oxygen tetrahedra, in addition to the usual oxygen octahedra that are typical of the perovskite structure. We then allow such a phase to relax within the *Imma* symmetry, the relaxation involving oxygen octahedra tilting about pseudocubic [100] and [010] directions and Co ions moving towards the center of oxygen tetrahedra.

Let us now pay attention to the four different oxygen tetrahedra shown in the bottom of Fig. 1, which we denote as T1, T2, T3, and T4. T1 and T2 belong to the same (001) oxygen tetrahedra layer, while T3 and T4 both occur in the subsequent (001) layer containing oxygen tetrahedra. As is the case for octahedral tilting in perovskites, if we choose a given tetrahedron and select a specific rotation about the *z* axis (e.g., clockwise), then the nearest corner-sharing tetrahedra belonging to the same (001) layer will rotate in the opposite way (e.g., anticlockwise) about the same out-of-plane axis. The different *z*-rotation patterns about T1, T2, T3, and T4 break the *Imma* symmetry and result in the following structural phases of brownmillerites: (1) the orthorhombic *Ima2* phase, when T1 and T2 rotate anticlockwise while T3 and T4 adopt a clockwise

TABLE I. Total energy E , in meV/f.u. (i.e., per nine atoms), and polarization P , in $\mu\text{C}/\text{cm}^2$, of the $\text{Sr}_2\text{Co}_2\text{O}_5$ and $\text{Ca}_2\text{Co}_2\text{O}_5$ BM oxides having G-type AFM spin orders in the different studied phases. The zero of energy corresponds to the predicted ground state in both of these systems. The main nontrivial modes of each structural phase are also provided in the first row.

		<i>Imma</i>	<i>Ima2</i>	<i>Pnma</i>	<i>Pbcm</i>	<i>Pmc2₁</i>
	Mode		Γ_4^-	X_4^-	Λ_3	Γ_4^- , Λ_3 , X_4^-
$\text{Sr}_2\text{Co}_2\text{O}_5$	E	253.2	87.0	2.6	61.0	0.0
	P	0.0	11.6	0.0	0.0	3.5
$\text{Ca}_2\text{Co}_2\text{O}_5$	E	473.3	69.2	0.0	24.5	1.8
	P	0.0	12.9	0.0	0.0	3.7

rotation, which constitutes an overall tetrahedra rotation pattern that we will term here as $- - + +$ and which corresponds to a mode with symmetry Γ_4^- ; (2) the orthorhombic *Pnma* phase when T1, T2, T3, and T4 all rotate in a clockwise fashion to form the $++ ++$ tilting pattern that is associated with a X_4^- mode; (3) another orthorhombic phase, but of the *Pbcm* space group, for the $+ - + -$ tetrahedra rotation pattern, associated to a Λ_3 mode; and (4) the orthorhombic *Pmc2₁* phase that occurs when three of the four tetrahedra rotate in the same fashion and in opposite way to the fourth tetrahedron, generating, e.g., the $++ - +$ tilting pattern for which all four tetrahedra rotate in a clockwise fashion, with the exception of T3 that rotates counterclockwise. Interestingly, the last pattern involves several phonon modes rather than a single one. As indicated in Table I, these simultaneous modes are Γ_4^- , X_4^- , and Λ_3 . It is important to note that both the *Ima2* and *Pmc2₁* space groups allow for the occurrence of a spontaneous in-plane electrical polarization as a result of their tilting pattern, unlike *Imma*, *Pnma*, and *Pbcm*, which are all paraelectric. Note also that the work of Young *et al.* [4] has already pointed out the existence of the *Imma*, *Ima2*, *Pnma*, and *Pbcm* phases in brownmillerites but overlooked the possibility of having a *Pmc2₁* state in these materials—probably because the *Imma*, *Ima2*, *Pnma*, and *Pbcm* structures are the result of the condensation of a single mode (in addition to the trivial Γ_1^+ symmetric distortion), unlike *Pmc2₁*. Note also that oxygen tetrahedral rotations have indeed been observed in various brownmillerites, such as $\text{Ca}(\text{Al}, \text{Fe})\text{O}_{2.5}$ [30], $\text{CaCrO}_{2.5}$ [31], $\text{CaFeO}_{2.5}$ [32], and $\text{SrFeO}_{2.5}$ [7,33].

Technically, we use 36-atom periodic supercells for investigating the *Ima2* and *Pnma* states and 72-atom supercells for *Pbcm* and *Pmc2₁*. The cell shape, volume, and atomic positions of all these supercells are optimized to relax the studied systems and phases. Table I reports the total energy of the relaxed *Imma*, *Ima2*, *Pnma*, *Pbcm*, and *Pmc2₁* states, as well as the corresponding values of the polarization in the case of *Ima2* and *Pmc2₁*, for $\text{Sr}_2\text{Co}_2\text{O}_5$ and $\text{Ca}_2\text{Co}_2\text{O}_5$. The paraelectric *Pnma* and polar *Pmc2₁* phases are the lowest-energy states in these two materials, with *Pnma* being the predicted ground state of $\text{Ca}_2\text{Co}_2\text{O}_5$ while it is *Pmc2₁* in $\text{Sr}_2\text{Co}_2\text{O}_5$. Note that, in both cases, the energy differences between the *Pnma* and *Pmc2₁* structures are minute, of 2–3 meV per formula unit of nine atoms. Table I also shows that the computed polarization of the predicted

$Pmc2_1$ ground state of $Sr_2Co_2O_5$ is $3.5 \mu C/cm^2$ in magnitude, therefore making $Sr_2Co_2O_5$ a multiferroic system since it also adopts a G-type antiferromagnetic ordering. Note that several conflicting phases have been suggested for $Sr_2Co_2O_5$. For instance, Muñoz *et al.* [28] proposed that the most stable phase at low temperature has the $Ima2$ symmetry, based on neutron powder-diffraction (NPD) and x-ray diffraction spectrum (XRD) measurements combined with calculations; in contrast, Sullivan *et al.* [29] either supported the $Pnma$ space group from electron microscopy or $Imma$ from their NPD data. Our calculations disagree with all these suggestions, since they predict a $Pmc2_1$ ground state. Such difficulty in determining the precise symmetry of the ground state experimentally may either arise from the similarity of all these phases as regards their XRD spectrum (see Fig. S1 of the SM [25]) or from the previous overlook that $Pmc2_1$ can also be a low-energy state in BM. Note also that the captions of Fig. S1 of the SM further discuss the exciting possibility that $Sr_2Co_2O_5$ can be a room-temperature multiferroic, while Fig. S5 and Table S2 of the SM report different magnetoelectric coupling effects in this compound.

To gain even more insight into this new $Pmc2_1$ state, let us now consider how the energy of these materials varies when the relaxed $Imma$ structure is distorted according to the most important modes. Up to fourth order, this energy can be written as (see SM [25] for more information)

$$\begin{aligned}
 E = E_0 &+ \gamma_{3000} Q_{\Gamma_1^+}^3 + \delta_{0211} Q_{\Lambda_3}^2 Q_{\Gamma_4^-} Q_{X_4^-} \\
 &+ \beta_{2000} Q_{\Gamma_1^+}^2 + \beta_{0200} Q_{\Lambda_3}^2 + \beta_{0020} Q_{\Gamma_4^-}^2 + \beta_{0002} Q_{X_4^-}^2 \\
 &+ \gamma_{1200} Q_{\Gamma_1^+} Q_{\Lambda_3}^2 + \gamma_{1020} Q_{\Gamma_1^+} Q_{\Gamma_4^-}^2 + \gamma_{1002} Q_{\Gamma_1^+} Q_{X_4^-}^2 \\
 &+ \delta_{4000} Q_{\Gamma_1^+}^4 + \delta_{0400} Q_{\Lambda_3}^4 + \delta_{0040} Q_{\Gamma_4^-}^4 + \delta_{0004} Q_{X_4^-}^4 \\
 &+ \delta_{2200} Q_{\Gamma_1^+}^2 Q_{\Lambda_3}^2 + \delta_{2020} Q_{\Gamma_1^+}^2 Q_{\Gamma_4^-}^2 + \delta_{2002} Q_{\Gamma_1^+}^2 Q_{X_4^-}^2 \\
 &+ \delta_{0220} Q_{\Lambda_3}^2 Q_{\Gamma_4^-}^2 + \delta_{0202} Q_{\Lambda_3}^2 Q_{X_4^-}^2 + \delta_{0022} Q_{\Gamma_4^-}^2 Q_{X_4^-}^2, \quad (1)
 \end{aligned}$$

where $Q_{\Gamma_1^+}$, Q_{Λ_3} , $Q_{\Gamma_4^-}$, and $Q_{X_4^-}$ represent the (dimensionless) amplitude of Γ_1^+ , Λ_3 , Γ_4^- , and X_4^- modes, respectively. α_{ijkl} , β_{ijkl} , γ_{ijkl} , and δ_{ijkl} are expansion coefficients (expressed in eV/72 atoms). $Q_{\Gamma_1^+} = Q_{\Lambda_3} = Q_{\Gamma_4^-} = Q_{X_4^-} = 1$ corresponds to the $Pmc2_1$ ground state, while the high-symmetry relaxed $Imma$ phase is characterized by $Q_{\Gamma_1^+} = Q_{\Lambda_3} = Q_{\Gamma_4^-} = Q_{X_4^-} = 0$. One can see, e.g., that Eq. (1) involves a linear-quadratic coupling (such as $Q_{\Gamma_1^+}^2 Q_{\Lambda_3}$) between Γ_1^+ and each of the other three modes, but also a biquadratic coupling (e.g., $Q_{\Gamma_4^-}^2 Q_{X_4^-}^2$) between any two modes. Equation (1) also possesses an even more complex coupling between the three nontrivial main modes responsible for the occurrence of the $Pmc2_1$ structure; such a coupling has of the form $Q_{\Lambda_3}^2 Q_{\Gamma_4^-} Q_{X_4^-}$. The only odd powers appearing in Eq. (1) are all involving Γ_1^+ , either via the aforementioned linear-quadratic coupling or via the energy solely associated with Γ_1^+ (that is, $Q_{\Gamma_1^+}^3$). As a result of these odd powers and aforementioned couplings, Eq. (1) predicts that the $Pmc2_1$ ground state should be 4 times degenerate, that is, $Pmc2_1$ phases for which $(Q_{\Gamma_1^+}, Q_{\Lambda_3}, Q_{\Gamma_4^-}, Q_{X_4^-})$ are equal to $(1,1,1,1)$, $(1,-1,-1,-1)$, $(1,-1,1,1)$ and $(1,1,-1,-1)$ should all have the same total energy. Additional density functional theory calculations we

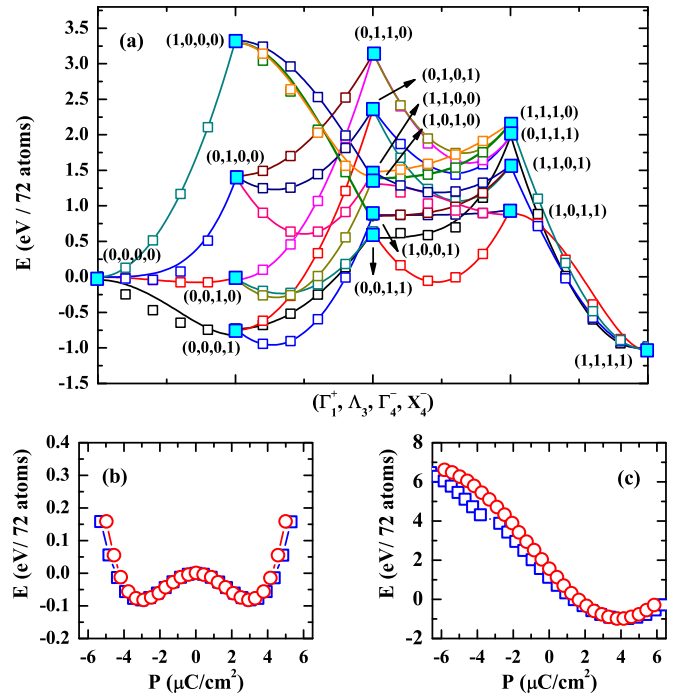


FIG. 2. Computed (a) transition paths between the relaxed $Imma$ state for which $(Q_{\Gamma_1^+}, Q_{\Lambda_3}, Q_{\Gamma_4^-}, Q_{X_4^-}) = (0, 0, 0, 0)$ and the polar $Pmc2_1$ state for which $(Q_{\Gamma_1^+}, Q_{\Lambda_3}, Q_{\Gamma_4^-}, Q_{X_4^-}) = (1, 1, 1, 1)$, (b) total energy versus polarization only considering the Γ_4^- mode (for which $Q_{\Gamma_1^+} = Q_{\Lambda_3} = Q_{X_4^-} = 0$), and (c) total energy versus polarization but in the case for which $Q_{\Gamma_1^+} = Q_{\Lambda_3} = Q_{X_4^-} = 1$, in G-type AFM-ordered $Sr_2Co_2O_5$. Solid lines in panel (a) show the fitting of the first-principles data by Eq. (1). The parameters resulting from this fitting are, in eV/72 atoms: $\gamma_{3000} = 0.26$, $\delta_{0211} = -4.60$, $\beta_{2000} = 3.08$, $\beta_{0200} = -0.10$, $\beta_{0020} = -0.28$, $\beta_{0002} = -1.56$, $\gamma_{1200} = -3.23$, $\gamma_{1020} = -1.86$, $\gamma_{1002} = -1.70$, $\delta_{4000} = -0.02$, $\delta_{0400} = 1.26$, $\delta_{0040} = 0.27$, $\delta_{0004} = 0.79$, $\delta_{2200} = -0.05$, $\delta_{2020} = -0.10$, $\delta_{2002} = -0.08$, $\delta_{0220} = 3.21$, $\delta_{0202} = 3.17$, and $\delta_{0022} = 2.33$. Blue and red data in panels (b) and (c) correspond to polarization being calculated by the Berry phase method and by the product of Born effective charges and ionic displacements, respectively. The zero of energy is chosen to be the energy of the relaxed $Imma$ state in all panels.

performed do confirm such degeneracy. Note that $Q_{\Gamma_4^-}$ and $Q_{X_4^-}$ have the same sign in these degenerate ground states because of the $Q_{\Lambda_3}^2 Q_{\Gamma_4^-} Q_{X_4^-}$ coupling, implying that a reversal of the polarization should be accompanied by the reversal of the X_4^- mode to end up in a $Pmc2_1$ minimum having the same energy.

We conducted first-principles simulations in $Sr_2Co_2O_5$ to obtain the total energy along various paths connecting the reference $Imma$ state to the polar $Pmc2_1$ ground state, as reported in Fig. 2(a). Fitting these latter simulations by Eq. (1) allows (i) to numerically check that our expression for the energy is indeed valid and (ii) to extract its expansion parameters in $Sr_2Co_2O_5$. These parameters are indicated in the captions of Fig. 2. As shown in Fig. 2(a), the distortions associated with the individual Γ_1^+ or Λ_3 modes typically increase the energy with respect to that of the relaxed $Imma$ phase, as consistent with the positive sign of the β_{2000} , γ_{3000} , and δ_{0400} coefficients. On the other hand, displacements originating from the Γ_4^- mode

only slightly lower the total energy with respect to that of the reference *Imma* structure (which is in line with the relatively small values of β_{0020} and δ_{0040}) and those associated with the X_4^- mode (which induces the paraelectric *Pnma* state) considerably lower the total energy—as consistent with the large negative β_{0002} parameter. Interestingly, *Pmc2*₁ is the predicted ground state of Sr₂Co₂O₅ because of the negative value of the coefficients related to the aforementioned linear-quadratic coupling (namely, $\gamma_{1200} = -3.23$, $\gamma_{1020} = -1.86$, and $\gamma_{1002} = -1.70$), but also because of the more complex coupling of the form $Q_{\Lambda_3}^2 Q_{\Gamma_4^-} Q_{X_4^-}$, for which the corresponding coefficient is $\delta_{0211} = -4.60$.

Let us now pay particular attention to the electrical polarization of the *Pmc2*₁ state, which is along a pseudocubic $\langle 110 \rangle$ direction. It originally arises from the Γ_4^- mode, which is polar in nature because of its associated $- - + +$ tetrahedral rotation pattern. As shown in Fig. 2(b), the polarization solely associated with the Γ_4^- mode (that is, when imposing $Q_{\Gamma_1^+} = Q_{\Lambda_3} = Q_{X_4^-} = 0$ in the calculations) gives rise to a double well in the energy curve which is characteristic of proper ferroelectrics. However, Eq. (1) tells us that this Γ_4^- mode can also couple with other modes, and that the resulting energy, to be denoted as E_{Polar} and gathering all the terms dependent on $Q_{\Gamma_4^-}$ (which is proportional to the magnitude of the polarization) is such as

$$E_{\text{Polar}} = \delta_{0211} Q_{\Gamma_4^-} Q_{\Lambda_3}^2 Q_{X_4^-} + Q_{\Gamma_4^-}^2 (\beta_{0020} + \gamma_{1020} Q_{\Gamma_1^+} + \delta_{2020} Q_{\Gamma_1^+}^2 + \delta_{0220} Q_{\Lambda_3}^2 + \delta_{0022} Q_{X_4^-}^2) + \delta_{0040} Q_{\Gamma_4^-}^4. \quad (2)$$

The second term of Eq. (2) indicates that the overall harmonic coupling affecting the polar distortion is renormalized by the interaction between the Γ_4^- mode and the other three modes. Such a coefficient goes from $\beta_{0020} = -0.28$ in the noninteracting case to $\beta_{0020} + \gamma_{1020} + \delta_{2020} + \delta_{0220} + \delta_{0022} = 3.30$ in the *Pmc2*₁ ground state. It thus evolves from slightly negative to a strongly positive value, indicating that linear-quadratic and biquadratic couplings have the overall effect of suppressing the polarization of the *Pmc2*₁ state. In fact, the reason why such a polar distortion survives is the first term of Eq. (2), i.e., the large negative δ_{0211} coefficient. Such a term is linear in the polarization (i.e., in $Q_{\Gamma_4^-}$), quadratic in Q_{Λ_3} , and linear in $Q_{X_4^-}$. The energetic coupling we discovered bears some resemblance with low-order energy in some commensurate phases [34]. It is thus different from (i) proper ferroelectricity (coefficient in front of $Q_{\Gamma_4^-}^2$ being negative); (ii) improper ferroelectricity (which would typically involve a coupling linear in polarization and quadratic in the main order parameter) [16]; (iii) triggered-type ferroelectricity, which would involve a negative bi-quadratic coupling between the polar distortion and the main order parameter [23,24]; and (iv) even the recently discovered hybrid improper ferroelectricity (for which polarization couples with two other modes via a trilinear coupling) [17–22]. One can thus assert that the polarization of the *Pmc2*₁ state, and the very stability of such a multimode phase, arises from a novel type of ferroelectricity because of $Q_{\Gamma_4^-} Q_{\Lambda_3}^2 Q_{X_4^-}$. The effect of this latter unusual coupling term is manifest in Fig. 2(c), which shows that the energy versus polarization curve exhibits a single well when imposing

$Q_{\Gamma_1^+} = Q_{\Lambda_3} = Q_{X_4^-} = 1$ along this curve. It is also interesting to realize that the difference in energy between the ferroelectric minimum of Fig. 2(c) and the relaxed *Imma* state is more than 10 times larger than that between the ferroelectric wells of Fig. 2(b) and the relaxed *Imma* state, while all these minima occur at a similar value of the polarization—that is, about 3–4 $\mu\text{C}/\text{cm}^2$. Such features arise from (i) the large magnitude of the negative δ_{0211} parameter (which quantifies the $Q_{\Gamma_4^-} Q_{\Lambda_3}^2 Q_{X_4^-}$ coupling); (ii) the small magnitude of the negative β_{0020} parameter (which represents the intrinsic instability of the Γ_4^- mode); and (iii) the relatively strong and positive sum of $\beta_{0020} + \gamma_{1020} + \delta_{2020} + \delta_{0220} + \delta_{0022}$ [which is the overall parameter associated with $Q_{\Gamma_4^-}^2$ in Eq. (2)]. Note that items (i)–(iii) are also found when determining the expansion parameters of Eq. (1) from simulations performed with the PBE functional using $U = 2.5$ eV, as shown in Fig. S4 and Table SI of the SM [25]. Note also that this value of 3–4 $\mu\text{C}/\text{cm}^2$ is between 1 and 2 orders of magnitude larger than the polarization of some improper ferroelectrics [35–38], while being about the same order as that of other improper ferroelectrics [39,40]. It is also about 1 order of magnitude smaller than the polarization of BaTiO₃, a prototypical proper ferroelectric [41]. It is also important to realize that Fig. 2(a) clearly shows that the condensation of the X_4^- mode alone leads to a significant decrease of the total energy with respect to that resulting from the sole condensation of Γ_1^+ , Λ_3 , or Γ_4^- , which demonstrates that X_4^- is the (main) primary order parameter of the transition from *Imma* to *Pmc2*₁. However, and as aforementioned, Fig. 2(b) further indicates that Γ_4^- is also unstable by itself, which can be thought to demonstrate that Γ_4^- is also an active order parameter. Moreover, Eqs. (1) and (2) and the resulting analysis of Fig. 2(a) reveal that our discovered novel quadratic-bilinear coupling (of the form $Q_{\Gamma_4^-} Q_{\Lambda_3}^2 Q_{X_4^-}$) is also essential to generate the *Pmc2*₁ structure. In other words, the transition from *Imma* to *Pmc2*₁ involves two (intrinsically unstable) order parameters as well as a novel energetic coupling, which further demonstrates its originality.

IV. SUMMARY

In summary, we have conducted and analyzed first-principles calculations on two different representatives of BM structure, i.e., Ca₂Co₂O₅ and Sr₂Co₂O₅. A previously overlooked polar *Pmc2*₁ state is stable and of low energy in these two magnetic compounds, and is even the ground state of Sr₂Co₂O₅, therefore making this compound multiferroic in nature. It is also striking that (i) the high-symmetry *Imma* phase of Sr₂Co₂O₅ has an intrinsic polar instability that is suppressed when incorporating all the biquadratic couplings between the polar Γ_4^- mode and the three nonpolar main modes of *Pmc2*₁; and (ii) that the occurrence of the polarization in the *Pmc2*₁ state in fact originates from a novel energetic coupling of the form $Q_{\Lambda_3}^2 Q_{\Gamma_4^-} Q_{X_4^-}$. Such a quadratic-bilinear coupling involving all three nontrivial modes of the *Pmc2*₁ structure differs from those that are typical of proper, improper, hybrid improper, and triggered kinds of ferroelectricity and is therefore indicative of a novel type of ferroelectricity. In fact, we numerically found (see Table S6 of the SM [25]) that such a ferroelectric state is of low energy in several BM structures, such as Ca₂Fe₂O₅ or Sr₂Fe₂O₅. Hence, it may be

possible to also stabilize it under some special conditions, such as applying electric fields or growing the samples on suitable substrates. We thus hope that the present study will motivate further theoretical and experimental studies on brownmillerites as a promising family for designing novel functional materials. Note, however, that our calculations do not preclude the possibility of structures that are longer in period than those studied here, or even incommensurate in brownmillerites.

ACKNOWLEDGMENTS

This work is supported by the National Natural Science Foundation of China (No. 11574220). H.T. is thankful

for the support of the State Scholarship Fund from the China Scholarship Council. Y.Y. and L.B. acknowledge ONR Grants No. N00014-12-1-1034 and No. N00014-17-1-2818. C.X. and S.O.S. also thank the Department of Energy, Office of Basic Energy Sciences, for support under Contract No. ER-46612 and DARPA Grant No. HR0011-15-2-0038 (under the MATRIX program), respectively. We also thank the Luxembourg National Research Fund for support through Grants No. INTER/MOBILITY/15/9890527 GREENOX (L.B. and J.I.) and No. FNR/P12/4853155/Kreisel COFERMAT (J.I.). The Arkansas High Performance Computing Center (AHPCC) is also acknowledged for the use of its supercomputers.

-
- [1] J. A. Kilner and M. Burriel, *Annu. Rev. Mater. Res.* **44**, 365 (2014).
 - [2] H. Jeon, W. S. Choi, M. D. Biegalski, C. M. Folkman, I.-C. Tung, D. D. Fong, J. W. Freeland, D. Shin, H. Ohta, M. F. Chisholm *et al.*, *Nat. Mater.* **12**, 1057 (2013).
 - [3] R. Waser and M. Aono, *Nat. Mater.* **6**, 833 (2007).
 - [4] J. Young and J. M. Rondinelli, *Phys. Rev. B* **92**, 174111 (2015).
 - [5] J. Young, E. J. Moon, D. Mukherjee, G. Stone, V. Gopalan, N. Alem, S. J. May, and J. M. Rondinelli, *J. Am. Chem. Soc.* **139**, 2833 (2017).
 - [6] Q. Lu and B. Yildiz, *Nano Lett.* **16**, 1186 (2016).
 - [7] A. Khare, D. Shin, T. S. Yoo, M. Kim, T. D. Kang, J. Lee, S. Roh, I.-H. Jung, J. Hwang, S. W. Kim *et al.*, *Adv. Mater.* **29**, 1606566 (2017).
 - [8] Q. Lu, Y. Chen, H. Bluhm, and B. Yildiz, *J. Phys. Chem. C* **120**, 24148 (2016).
 - [9] N. Lu, P. Zhang, Q. Zhang, R. Qiao, Q. He, H.-B. Li, Y. Wang, J. Guo, D. Zhang, Z. Duan *et al.*, *Nature (London)* **546**, 124 (2017).
 - [10] H.-B. Li, N. Lu, Q. Zhang, Y. Wang, D. Feng, T. Chen, S. Yang, Z. Duan, Z. Li, Y. Shi, W. Wang, W.-H. Wang, K. Jin, H. Liu, J. Ma, L. Gu, C. Nan, and P. Yu, *Nat. Commun.* **8**, 2156 (2017).
 - [11] Y. Yang, C. Ma, M. Liu, H. J. Zhao, Y. Lin, C. Chen, and L. Bellaiche, *Phys. Rev. B* **95**, 165132 (2017).
 - [12] W. Eerenstein, N. Mathur, and J. F. Scott, *Nature (London)* **442**, 759 (2006).
 - [13] S. M. Young, F. Zheng, and A. M. Rappe, *Phys. Rev. Appl.* **4**, 054004 (2015).
 - [14] J. Scott, *Nat. Mater.* **6**, 256 (2007).
 - [15] R. Nechache, C. Harnagea, S. Li, L. Cardenas, W. Huang, J. Chakrabarty, and F. Rosei, *Nat. Photonics* **9**, 61 (2015).
 - [16] A. P. Levanyuk and D. G. Sannikov, *Sov. Phys. Usp.* **17**, 199 (1974).
 - [17] H. J. Zhao, J. Íñiguez, W. Ren, X. M. Chen, and L. Bellaiche, *Phys. Rev. B* **89**, 174101 (2014).
 - [18] E. Bousquet, M. Dawber, N. Stucki, C. Lichtensteiger, P. Hermet, S. Gariglio, J.-M. Triscone, and P. Ghosez, *Nature (London)* **452**, 732 (2008).
 - [19] N. A. Benedek and C. J. Fennie, *Phys. Rev. Lett.* **106**, 107204 (2011).
 - [20] J. M. Rondinelli and C. J. Fennie, *Adv. Mater.* **24**, 1961 (2012).
 - [21] J. Young and J. M. Rondinelli, *Chem. Mater.* **25**, 4545 (2013).
 - [22] A. T. Mulder, N. A. Benedek, J. M. Rondinelli, and C. J. Fennie, *Adv. Funct. Mater.* **23**, 4810 (2013).
 - [23] J. Holakovský, *Phys. Status Solidi B* **56**, 615 (1973).
 - [24] I. A. Kornev and L. Bellaiche, *Phys. Rev. B* **79**, 100105 (2009).
 - [25] See Supplemental Material at <http://link.aps.org/supplemental/10.1103/PhysRevMaterials.2.084402> for details about the methods used as well as additional information.
 - [26] W. Kohn and L. J. Sham, *Phys. Rev.* **140**, A1133 (1965).
 - [27] J. P. Perdew, A. Ruzsinszky, G. I. Csonka, O. A. Vydrov, G. E. Scuseria, L. A. Constantin, X. Zhou, and K. Burke, *Phys. Rev. Lett.* **100**, 136406 (2008).
 - [28] A. Muñoz, C. de la Calle, J. A. Alonso, P. M. Botta, V. Pardo, D. Baldomir, and J. Rivas, *Phys. Rev. B* **78**, 054404 (2008).
 - [29] E. Sullivan, J. Hadermann, and C. Greaves, *J. Solid State Chem.* **184**, 649 (2011).
 - [30] A. Colville and S. Geller, *Acta. Crystallogr., Sect. B: Struct. Crystallogr. Cryst. Chem.* **27**, 2311 (1971).
 - [31] A. M. Arevalo-Lopez and J. P. Attfield, *Dalton Trans.* **44**, 10661 (2015).
 - [32] K. Gupta, S. Singh, M. Ceretti, M. Rao, and W. Paulus, *Phys. Status Solidi A* **210**, 1771 (2013).
 - [33] H. D'Hondt, A. M. Abakumov, J. Hadermann, A. S. Kalyuzhnaya, M. G. Rozova, E. V. Antipov, and G. Van Tendeloo, *Chem. Mater.* **20**, 7188 (2008).
 - [34] K. Parlinski, *J. Phys. C* **18**, 5667 (1985).
 - [35] C. Xu, Y. Li, B. Xu, J. Íñiguez, W. Duan, and L. Bellaiche, *Adv. Funct. Mater.* **27**, 1604513 (2017).
 - [36] T. Kimura, T. Goto, H. Shintani, K. Ishizaka, T.-h. Arima, and Y. Tokura, *Nature (London)* **426**, 55 (2003).
 - [37] S. Sawada, Y. Shiroishi, A. Yamamoto, M. Takashige, and M. Matsuo, *J. Phys. Soc. Jpn.* **43**, 2099 (1977).
 - [38] K. Aiki, K. Hukuda, and O. Matumura, *J. Phys. Soc. Jpn.* **26**, 1064 (1969).
 - [39] H. J. Zhao, W. Ren, Y. Yang, J. Íñiguez, X. M. Chen, and L. Bellaiche, *Nat. Commun.* **5**, 4021 (2014).
 - [40] N. Fujimura, T. Ishida, T. Yoshimura, and T. Ito, *Appl. Phys. Lett.* **69**, 1011 (1996).
 - [41] G. Kwei, A. Lawson, S. Billinge, and S. Cheong, *J. Phys. Chem.* **97**, 2368 (1993).